

Apelin Is Required for Non-Neovascular Remodeling in the Retina

Jenny A.G. McKenzie,* Marcus Fruttiger,*
Sabu Abraham,* Clemens A.K. Lange,^{†‡}
Jay Stone,* Pranita Gandhi,* Xiaomeng Wang,*
James Bainbridge,[†] Stephen E. Moss,* and
John Greenwood*

From the Departments of Cell Biology* and Genetics,[†] University College London Institute of Ophthalmology, London, United Kingdom; and the University Eye Hospital Freiburg,[‡] Freiburg, Germany

Retinal pathologies are frequently accompanied by retinal vascular responses, including the formation of new vessels by angiogenesis (neovascularization). Pathological vascular changes may also include less well characterized traits of vascular remodeling that are non-neovascular, such as vessel pruning and the emergence of dilated and tortuous vessel phenotypes (telangiectasis). The molecular mechanisms underlying neovascular growth versus non-neovascular remodeling are poorly understood. We therefore undertook to identify novel regulators of non-neovascular remodeling in the retina by using the dystrophic Royal College of Surgeons (RCS) rat and the retinal dystrophy 1 (RD1) mouse, both of which display pronounced non-neovascular remodeling. Gene expression profiling of isolated retinal vessels from these mutant rodent models and wild-type controls revealed 60 differentially expressed genes. These included the genes for apelin (*Apln*) and for its receptor (*Aplnr*), both of which were strongly up-regulated in the mutants. Crossing RD1 mice into an *Apln*-null background substantially reduced vascular telangiectasia. In contrast, *Apln* gene deletion had no effect in two models of neovascular pathology [laser-induced choroidal neovascularization and the very low density lipoprotein receptor (*Vldlr*)-knockout mouse]. These findings suggest that in these models apelin has minimal effect on sprouting retinal angiogenesis, but contributes significantly to pathogenic non-neovascular remodeling. (*Am J Pathol* 2012, 180:399–409; DOI: 10.1016/j.ajpath.2011.09.035)

Development of the retinal vasculature is initiated by blood vessels in the optic nerve head. These vessels form sprouts that develop into a primitive vascular plexus by the process

of angiogenesis.¹ Initially, a simple network is established at the inner surface of the retina; from there, vascular sprouts subsequently penetrate the retina to form a second, deeper plexus. To generate the patterned and hierarchically branched network characteristic of the mature retinal vasculature, these primary vascular plexuses undergo extensive remodeling to achieve the final vascular configuration. Much research has focused on sprouting angiogenesis in the retina because of its link to pathology in the adult (referred to as neovascularization), including blinding complications in diseases such as diabetic retinopathy or age-related macular degeneration. Various trophic factors have been identified as important regulators of the process, with the vascular endothelial growth factors (VEGFs) and their receptors being viewed as critical components.² Indeed, therapeutic targeting of VEGF in ocular angiogenesis has resulted in improved clinical outcome in a number of sight-threatening conditions. Nevertheless, other factors, including transforming growth factor β 1 (TGF- β 1), basic fibroblast growth factor (bFGF), insulin-like growth factor 1 (IGF-1), platelet-derived growth factor (PDGF), and angiopoietin are also thought to contribute, either by modifying the VEGF response or by independently regulating the remodeling of existing vessels.

Non-neovascular remodeling is a characteristic of many sight-threatening retinal diseases. For instance, adult vessels can become telangiectatic (tortuous and dilated) in diseases such as macular telangiectasia,³ diabetic retinopathy,⁴ Coats' disease,⁵ radiation-induced retinal telangiectasia,⁶ and ataxia-telangiectasia.⁷ Similarly, in the retinitis pigmentosa (RP) family of diseases the degeneration of photoreceptors leads to remodeling

Supported by the Lowy Medical Research Institute, Ltd. (The Macular Telangiectasia Project), The Wellcome Trust, NIHR Biomedical Research Centre for Ophthalmology at Moorfields Eye Hospital, and the UCL Institute of Ophthalmology.

Accepted for publication September 27, 2011.

S.E.M. and J.G. contributed equally to the present work and each is considered senior author.

Supplemental material for this article can be found at <http://ajp.amjpathol.org> or at doi: 10.1016/j.ajpath.2011.09.035.

Address reprint requests to John Greenwood, Ph.D., UCL Institute of Ophthalmology, 11-43 Bath Street, London EC1V 9EL, UK. E-mail: j.greenwood@ucl.ac.uk.

and attenuation of the retinal vasculature.⁸ Morphologically similar patterns of non-neovascular remodeling are also observed in rodent models with photoreceptor degeneration, such as the Royal College of Surgeons (RCS) rat and the retinal degeneration 1 (RD1) mouse. In the RCS rat, retinal degeneration occurs because of a mutation in the *Mertk* gene, resulting in defective phagocytosis of the outer segments and photoreceptor cell death.^{9,10} The deeper plexus of the retinal vasculature subsequently becomes leaky and develops telangiectatic vessels.¹¹ In the RD1 mouse, rapid photoreceptor loss due to the presence of a mutation within the photoreceptor cGMP phosphodiesterase gene begins at postnatal day 8 (P8), with complete rod photoreceptor atrophy occurring by 4 weeks of age.^{12,13} This mutation also results in accompanying vascular atrophy. Vessels develop normally up to P12, but loss of capillaries within the deep vascular plexus follows, with subsequent appearance of telangiectatic vessels.^{14,15} The remodeling of existing vessels, such as the formation of telangiectasia, is clearly an important phenomenon that contributes to pathogenesis in a number of ocular and nonocular diseases. Although factors that contribute to developmental remodeling have been identified,¹⁶ those responsible for driving non-neovascular pathogenic modifications remain poorly defined.

In the present study, we investigated non-neovascular remodeling in two rodent models with retinal degenerative disease, the RCS rat and the RD1 mouse. Having established that the vascular changes, including the development of telangiectatic vessels, are non-neovascular and anatomically similar in both models, we embarked on gene expression analysis of isolated retinal microvascular fragments to identify candidate genes contributing to the process. A group of differentially expressed genes were identified, of which two [apelin (*Apln*) and its receptor (*Aplnr*)] were investigated further to establish their potential role in non-neovascular remodeling.

In the retina, *Aplnr* transcripts were uniquely expressed by endothelial and/or associated mural cells, whereas *Apln* was expressed predominantly by vessels but also other cells of the retina. Analysis of *Apln*-knockout mice revealed fewer radial veins and arteries and an increase in arteriovenous crossover. Furthermore, during retinal vascular development, radial veins failed to remodel into deep drainage venules in the *Apln*-knockout mice. In RD1 mice lacking the apelin gene, there was a similar failure to develop these deep drainage venules. Crucially, however, there was also a significant reduction in pathogenic telangiectatic vessels arising in the intermediate vascular plexus. These data indicate a key role for apelin in both developmental and pathogenic non-neovascular remodeling.

Materials and Methods

Animals

RD1 mice¹² and *Vldlr*^{-/-} mice¹⁷ were purchased from the Jackson Laboratory (Bar Harbor, ME). Control C57BL/6J mice were purchased from Harlan Laboratories (Blackthorn, UK). RCS dystrophic and congenic rats were bred

from an established in-house colony; the *Apln*-knockout mice were a generous gift from Dr. J.M. Penninger, Vienna, Austria.¹⁸ Double-mutant mice were generated by crossing an *Apln*-knockout mouse with an RD1 mouse to generate heterozygote offspring ($R^{-/+}/A^{-/+}$). These were crossed, and the resultant offspring were genotyped to identify animals that were both homozygous RD1 mutants and heterozygous *Apln* mutants ($R^{-/-}/A^{-/+}$). These mice were then crossed to generate RD1 homozygous mutants that were also either homozygous wild type for *Apln* ($R^{-/-}/A^{+/+}$) or homozygous mutant for *Apln* ($R^{-/-}/A^{-/-}$). The same procedure was applied to generate double-*Vldlr* and *Apln*-knockout mice. All experiments were performed in accordance with the Animals (Scientific Procedures) Act and ethically approved by the UK Home Office.

Vessel Isolation

Rat or mouse retinas were enzymatically digested in collagenase/dispase (1 mg/mL; Roche, Welwyn, UK) and DNase (20 U/mL; Ambion, Warrington, UK) at 37°C for 45 to 60 minutes. The microvessels were extracted using either anti-mouse or anti-rat PECAM-1 antibodies (BD Bioscience, Oxford, UK, and AbD Serotec, Kidlington, UK, respectively), followed by either sheep anti-mouse or sheep anti-rat IgG-conjugated magnetic beads (Dyna-bead; Invitrogen, Paisley, UK) and magnetic separation. The bead-bound vessels (vessel-enriched) and vessel-depleted fractions were separately lysed for Western blotting or for RNA extraction and analysis.

Immunohistochemistry

Bead-bound vessels were paraformaldehyde-fixed and then dried onto SuperFrost microscope slides (VWR International, Leicestershire, UK). They were then stained with anti-collagen IV (AbD Serotec), caveolin 1 (BD Biosciences), fibronectin (Millipore-Chemicon International, Temecula, CA), or α -smooth muscle actin (ASMA) (Sigma-Aldrich, Dorset, UK) antibodies, followed by incubation with their respective Alexa Fluor 555- and 488-labeled secondary antibodies (Invitrogen).

Retinal whole mounts were fixed and stained as described previously.¹ Briefly, eyes were rapidly fixed in 2% paraformaldehyde before retinal dissection in PBS and refixation in 100% ice-cold methanol overnight at -20°C. Retinas were rehydrated, blocked in blocking buffer (3% Triton-X-100, 1% Tween-20, 0.5% bovine serum albumin in PBS) and incubated overnight with either rabbit-anti-mouse collagen IV (AbD Serotec) or fluorescein isothiocyanate-isolectin B4 (Vector Laboratories, Peterborough, UK). Retinas were then washed before incubation with Alexa Fluor 488-labeled secondary antibodies (Invitrogen) and mounted in Mowiol 4-88 reagent (Merck Chemicals, Nottingham, UK) and examined by fluorescence (Leica) or confocal (Zeiss LSM 510) light microscopy. For quantification of telangiectatic vessels, the number of 360-degree turns in the vessels were counted per retina. For evaluating the vascular growths in the *Vldlr*^{-/-} animals, the numbers of collagen IV-

positive vascular tufts on the outer retina were counted per retina and averaged.

Laser-Induced Choroidal Neovascularization

Laser-induced choroidal neovascularization (CNV) and quantification using fundus fluorescein angiography was performed as described previously.¹⁹ Three laser lesions per eye were delivered at two to three disk diameters away from the optic nerve head with a slit-lamp-mounted diode laser system (Keeler SL-16, Windsor, UK; wavelength: 680 nm; laser settings: 210 mW power, 100 ms duration, 100 μ m spot diameter). At 2 weeks after laser induction, *in vivo* fundus fluorescein angiography was performed, and images from the early phase (90 seconds after fluorescein injection) and late phase (7 minutes) were obtained using a Kowa Genesis small animal fundus camera with appropriate filters (Kowa Optimed, Torrance, CA). The pixel area of CNV-associated hyperfluorescence was quantified for each lesion using ImageJ version 1.44i image analysis software (NIH, Bethesda, MD). To quantify the volume of the CNV lesions, whole mounts of the eye cup were prepared by carefully peeling off the neural retina and exposing the CNV attached to the retinal pigment epithelium (RPE). CNV lesions were immunostained for PECAM-1 using the protocol described above for immunohistochemistry. Confocal sections were obtained using a Zeiss LSM 710 upright confocal microscope using a 40 \times water immersion plan Apochromat lens. Z-stacks were captured and three-dimensional images were reconstructed, followed by surface rendering, using Imaris software version 7.3 (Bitplane, Zurich, Switzerland). CNV volume was calculated using the Imaris measurement module.

SDS-PAGE and Western Blotting

Proteins were separated by SDS-PAGE, transferred onto a nitrocellulose membrane by wet transfer, bovine serum albumin blocked, and incubated with goat anti-VE-cadherin (Santa Cruz Biotechnology, Heidelberg, Germany), followed by HRP-conjugated secondary antibodies (Santa Cruz Biotechnology). Blots were developed using luminescent substrates (Roche, Welwyn, UK). The gel was subsequently stained using Coomassie Blue and destained to visualize the bands. Densitometry was performed using ImageJ software version 1.44i.

Quantitative Real-Time PCR

RNA was extracted using TRIzol reagent (Invitrogen), followed by an RNeasy clean-up (Qiagen, West Sussex, UK). RNA was DNase-treated and reverse-transcribed using Qiagen QuantiTect kits, and real-time PCR was performed using Power SYBR PCR master mix (Applied Biosystems, Paisley, UK). The following primers were used: mouse VE-cadherin (Fwd: 5'-CATAACAACAATGACAACACC-3', Rev: 5'-GATGATCAGCAAGGTAATCAC-3'); PDGFR- α (Fwd 5'-TGTAGACTTGGAGAACTACTGC-3', Rev: 5'-CGCTCTCACACTTACC-3') rhodopsin (Fwd: 5'-TGGTGGTCTGTTGCTCTC-3', Rev: 5'-

GCTGCTCTATCACATTCCC-3'); desmin (Fwd: 5'-TCATCGCCCTTCCCCTTC-3', Rev: 5'-GTCCACAACTCGGTCCTG-3') APLNR (Fwd: 5'-GGGAGTAAGTTTGGGAAAGAG-3', Rev: 5'-TGGGAATATGTCTTGTCCCTGG-3'); APLN (Fwd: 5'-GGCCTTCTCCGTCTTTGTGCG-3', Rev: 5'-CCCTCTTGTGCTTCTATCTCTCC-3'); PECAM1 (Fwd: 5'-GCCAGTCACTTGAAGACAGACC-3', Rev: 5'-TGGAACGGAAAGGAAGATCAAGG-3'); β -actin (Fwd: 5'-TCCAAGTATCCATGAAATAAGTGG-3', Rev: 5'-GCAGTACATAATTTACACAGAAGC-3'); VEGF (Fwd: 5'-GACTTGTGTTGGGAGGAGGA-3', Rev: 5'-TCTGGAAGTGAGCCAA-TGTG-3'). Rat APLNR (Fwd: 5'-TTGGTCTTCTCTGTCCAGGAC-3', Rev: 5'-GTCACCTTTACACACCTTACC-3'); APLN (Fwd: 5'-CGTGTAGGGAGGTGAGTGCTTGATC-3', Rev: 5'-CGAACAGATGCCAAAGGACTTAAAGGG-3'); β -actin (Fwd: 5'-ATCGTGCCTGACATTAAG-3', Rev: 5'-GCCACAGGATTCCATACC-3'); VEGF (Fwd: 5'-GGTGACCAAGCACGGTGGTCC-3', Rev: 5'-TAAGAAAGGACGAAAGACCACACCGG-3'). Genotyping primers were as follows: RD1 mutant²⁰: 5'-GTAAACAGCAAGAGGCTTTATTGGGAAC-3', RD1 wild-type: 5'-TACCCACCTTCTAATTTTCTCAGC-3', RD1 common: 5'-TGACAATTACTCCTTTCCCTCAGTCTG-3'; APLN mutant: 5'-GACAGTTTCTCTAACTCAAAGGGCC-3', APLN wild type: 5'-GCTTCCTTCTTAGTCTGTTCCA-3', APLN common: 5'-ATGTCTGGGTGTAGGTCCATAAAGG-3' (MWG Biotech, London, UK).

Microarrays

Microvessels were isolated from six nondystrophic and six dystrophic RCS rat retinas, all rats at 5 months of age. The RNA was extracted, amplified, and labeled for microarray analysis using an Affymetrix two-cycle labeling kit according to the manufacturer's instructions (Affymetrix, High Wycombe, UK). Similarly, RNA was extracted from isolated vessels from 12 C57BL/6J mice (15 weeks of age) and 12 RD1 mice (18 weeks of age) and processed for microarray analysis. This was repeated four times for each animal model, providing RNA for four chips per animal model. RNA quality was checked using an Agilent Technologies (Santa Clara, CA; Waldbronn, Germany) bioanalyzer before hybridization to Affymetrix mouse 430.2 or rat 230.2 gene arrays at the UCL Wolfson Institute and UCL Institute for Child Health Microarray Facility. The data were analyzed using Bioconductor 2.0 and RGui software version 2.5.1 as described previously.²¹

Statistical Analysis

Paired and unpaired data were analyzed using a Student's *t*-test. A maximum *P* value of 0.05 was considered significant. For the microarrays, statistical analysis was done using the RGui LIMMA software package version 2.5.1 as described previously.²¹ A false discovery rate statistical post hoc test ($q \leq 0.05$) was used for the RD1 mouse, and a log₂ fold change of ≥ 2 with a *P* value of ≤ 0.01 was used for the RCS rat.

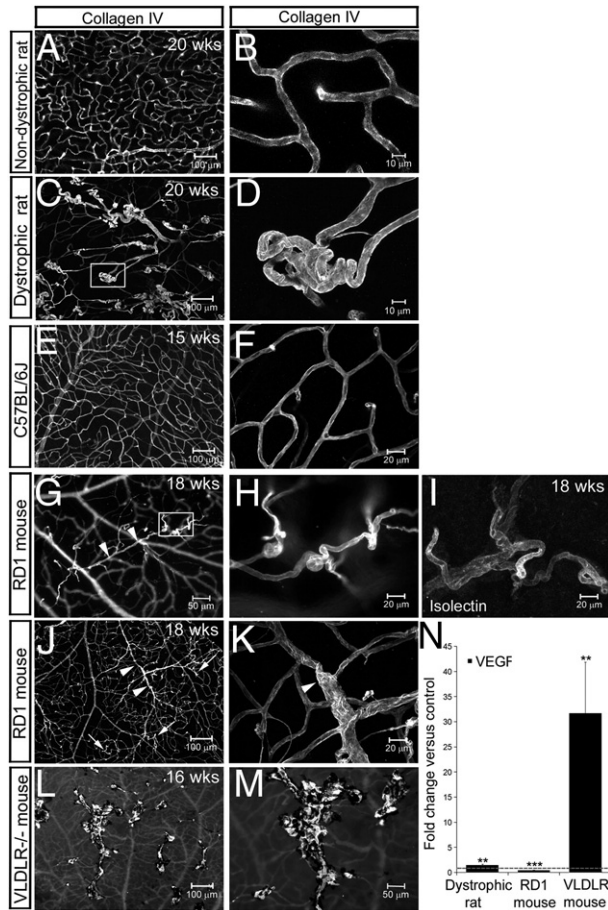


Figure 1. Vascular remodeling in the RCS rat and the RD1 mouse. **A** and **B**: Nondystrophic RCS rat (20 weeks of age). **C** and **D**: Dystrophic RCS rat (20 weeks of age). **E** and **F**: C57BL/6J mouse (15 weeks of age). **G–K**: RD1 mouse (4.5 months). **L** and **M**: *Vldlr*^{-/-} mouse (16 weeks of age). Retinas were flat-mounted, vessels stained for collagen IV (**A–H** and **J–M**) or isolectin B4 (**D**) and viewed from the outer retina. **Arrowheads** in **G** indicate a tortuous vessel arising from the intermediate plexus (shown at higher magnification in **H**). In **J** and **K**, a remodeled radial vein is shown (**arrowheads**), associated with telangiectatic vessels (**arrows**). **N**: VEGF gene expression was measured in RCS rats, RD1 mice, and *Vldlr*^{-/-} mice by qPCR, relative to congenic RCS rats or C57BL/6J mice. Data are expressed as means ± SEM (*n* = 3). **P* ≤ 0.05; ***P* ≤ 0.01; ****P* ≤ 0.001, Student's *t*-test. Scale bars: 100 μm (**A**, **C**, **E**, **J**, and **L**); 50 μm (**G** and **M**); 20 μm (**F**, **H**, **I**, and **K**); 10 μm (**B** and **D**).

Results

RCS Dystrophic Rats and RD1 Mice Display Similar Vascular Remodeling

Detailed examination of the retinal vasculature of RCS dystrophic rats and RD1 mice was performed to establish the pattern of vascular remodeling in these animals. The retinas were flat-mounted and examined by immunostaining for collagen IV or isolectin B4. Compared with non-dystrophic RCS rats (Figure 1, A and B), the dystrophic RCS rat at 5 months of age had substantial retinal thinning due to photoreceptor degeneration, as well as extensive vascular abnormalities across the outer retina (Figure 1, C and D). Vessels from the deeper plexus had remodeled into telangiectatic vascular complexes that frequently consisted of length-expanded capillaries, folded in a corkscrew-like fashion. In some instances, these com-

plexes were directly associated with the RPE. These observations are consistent with previous reports.^{11,22}

In 4.5-month-old RD1 mice, we observed morphologically similar telangiectatic vessels extending from the remaining neuroretina toward the subretinal space (Figure 1, G and H), which were absent in wild-type C57BL/6J mice (Figure 1, E and F). Some of the telangiectatic vascular remodeling occurred on capillaries from the intermediate to deeper plexus (Figure 1, G and H) and some on vessels linked to drainage veins in the deeper plexus (Figure 1, J and K). Similar abnormalities have been reported previously and are most probably the precursors to RPE-associated vascular complexes observed from 6 months of age.¹⁵ At the earlier time points investigated, no association of vessels with the RPE was observed. The telangiectatic vessels stained positively for isolectin B4 (Figure 1I), demonstrating that they contained viable endothelial cells and were not acellular vessel ghosts. Furthermore, isolectin staining did not reveal any evidence of filopodia or vascular sprouting during this phase of vascular alteration, confirming that these vascular abnormalities do not form by sprouting angiogenesis but by non-neovascular remodeling.

Consistent with this observation, whole-retina quantitative PCR (qPCR) for VEGF on the RCS rat and RD1 mouse (at 5 months and 4.5 months of age, respectively) revealed only small changes in transcript expression, relative to the wild type (Figure 1N). To compare VEGF levels in the RCS rat and RD1 mouse with a rodent model of retinal neovascularization, we measured VEGF mRNA expression in the *Vldlr*^{-/-} mouse.^{17,23} In this mouse, which models retinal angiomatous proliferation, there is marked intraretinal neovascularization commencing from approximately P14 and continuing through to approximately P30. By 4 months of age, a portion of these abnormalities appear as plaques containing associated RPE on the outer retina (Figure 1, L and M).²⁴ We therefore evaluated whole-retina VEGF transcript expression by qPCR at P21 and observed a substantially greater fold change in VEGF expression, relative to the RCS rat or RD1 mouse (Figure 1N). In conjunction with the absence of tip cells, as judged by a lack of endothelial cell filopodia, these results suggest that VEGF-induced neovascularization is unlikely to be a major contributor to the observed remodeling of vessels in the RD1 mouse and RCS rat.

Differentially Expressed Genes in Retinal Microvessels of the RCS Rat and RD1 Mouse

Irrespective of disease causation, we hypothesize that downstream non-neovascular pathogenic changes are likely to be mediated by common mechanisms. To gain insight into the transcriptional programming that drives such vascular abnormalities, retinal microvessel fragments were purified from the retina of the RCS and RD1 mouse using anti-PECAM-1 magnetic beads (see Supplemental Figure S1A at <http://ajp.amjpathol.org>). Vessel-enriched and vessel-depleted fractions were obtained and examined by phase contrast and epifluorescent microscopy (see Supplemental Figure S1B <http://ajp>).

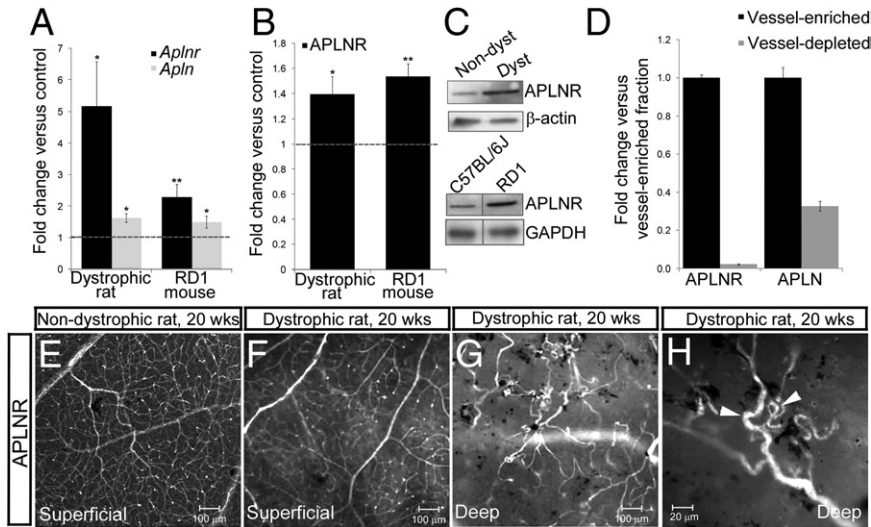


Figure 2. *Aplnr* and *Aplin* are increased in the RCS and RD1 rodent retina. **A:** *Aplnr* and *Aplin* expression as measured by qPCR in retinal extracts of RCS dystrophic rats ($n = 3$), relative to congenic RCS rats ($n = 3$), both 20 weeks of age, and of RD1 mice ($n = 3$), relative to wild-type C57BL/6J mice ($n = 3$), both 4.5 months of age. **B:** Protein expression of *Aplnr* in RCS dystrophic versus nondystrophic rat retina ($n = 4$) and in RD1 versus C57BL/6J mouse retina ($n = 4$). **C:** Representative findings of densitometry performed on three independent Western blots. **D:** Vessels were purified from mouse retinas and the vessel-enriched and vessel-depleted fractions were analyzed for *Aplnr* and *Aplin* expression by qPCR. Data are expressed as means \pm SEM ($n = 3$). * $P \leq 0.05$; ** $P \leq 0.01$, Student's *t*-test. **E–H:** Congenic (**E**) and dystrophic (**F–H**) RCS rat retinas were flat-mounted and immunostained for *Aplnr*. At higher magnification (**H**), *Aplnr* staining is visible in telangiectatic vessels (arrowheads). Scale bars: 100 μ m (**E–G**); 20 μ m (**H**).

ajp.amjpathol.org), and qPCR and Western blotting confirmed good vessel recovery and substantial enrichment of endothelial cell markers (see Supplemental Figure S1, C and D, at <http://ajp.amjpathol.org>). To test whether the vessel-enriched fraction contained other cell types besides endothelial cells, we performed qPCR with primers for the pericyte marker desmin, the glial marker PDGFR α , and the photoreceptor marker rhodopsin. The resulting data revealed contamination of glial cells, minor contamination by pericytes, but virtually no contamination from photoreceptors (see Supplemental Figure S2, A–C, at <http://ajp.amjpathol.org>).

Global gene expression analysis was then undertaken to identify genes in the endothelial-enriched fractions that may contribute to retinal non-neovascular remodeling in the RD1 mouse and RCS rat. Microarray analysis followed by false discovery rate statistical post hoc test with an adjusted P value of ≤ 0.05 revealed 3270 genes that were differentially regulated in the RD1 mouse. Reducing the stringency for the RCS rat by removing the post hoc test and using a fold change cutoff of ≥ 2 and a P value of ≤ 0.01 revealed 341 differentially regulated genes. Of these, 60 transcripts were common to the RD1 mouse and the RCS rat (see Supplemental Table S1 at <http://ajp.amjpathol.org>). Of the differentially regulated genes, the small secreted signaling peptide apelin (*Aplin*) and its receptor (*Aplnr*), both of which have previously been implicated in vascular development and pathology,^{25–29} were significantly up-regulated. Also up-regulated were adrenomedullin (*Adm*) and plasmalemma vesicle associated protein (*Plvap*); these are vascular-associated genes that have the potential to affect vascular function. Other genes found to be up-regulated included glial fibrillary acidic protein (*Gfap*) and the GABA_A receptor (*Gabra1*) derived from contaminating astroglia and neurons, respectively. Notably, the GABA_A receptor has been implicated in vascular remodeling in the brain.³⁰ However, many of the genes lacked any obvious functional connection to the vasculature. Furthermore, many of the down-regulated genes most likely resulted from the loss of contaminating photoreceptors

in the degenerate retinas (ie, phosducin, recoverin, and retbindin, among others). Because of the increasingly prevalent notion that apelin and its receptor affect vascular development and pathology, *Aplin* and *Aplnr* were chosen for further analysis.

Apelin and Its Receptor Are Up-Regulated in the Retinal Vasculature of the RCS Rat and RD1 Mouse

The microarray gene expression profiling of the dystrophic RCS rat and RD1 mouse retinal vasculature revealed an increase in the expression of *Aplnr* by 2.7-fold and 5.7-fold and of *Aplin* by 8.9-fold and 2.9-fold, respectively (see Supplemental Table S1 at <http://ajp.amjpathol.org>). To validate the microarray gene expression data, we undertook qPCR analysis on RNA isolated from total mouse and rat retinas. In agreement with the microarray results, a statistically significant increase in *Aplin* and *Aplnr* expression was observed in both animal models (Figure 2A). To establish whether the observed increase in retinal *Aplnr* mRNA in the animal models resulted in an increase in protein expression, *Aplnr* levels from whole-retina lysates of the RCS rat and RD1 mouse were evaluated by Western blot analysis. In both animal models, we detected a significant increase in *Aplnr*, relative to control levels (Figure 2, B and C). To determine whether expression in the retina was restricted to the vasculature we analyzed by qPCR the vessel-enriched and the vessel-depleted fractions of mouse retinal preparations. *Aplnr* expression was restricted to the vessel-enriched sample, indicating that the receptor is not expressed by cells of the neural retina. However, although *Aplin* expression was predominantly vascular, it was also observed in the vessel-depleted fraction (Figure 2D) suggesting that other cells, such as Müller glia, are also a potential source of the ligand. The expression of *Aplnr* was then confirmed by immunohistochemistry in the RCS rat, with a vascular pattern of staining observed in both congenic and dystrophic animals (Figure 2, E–H).

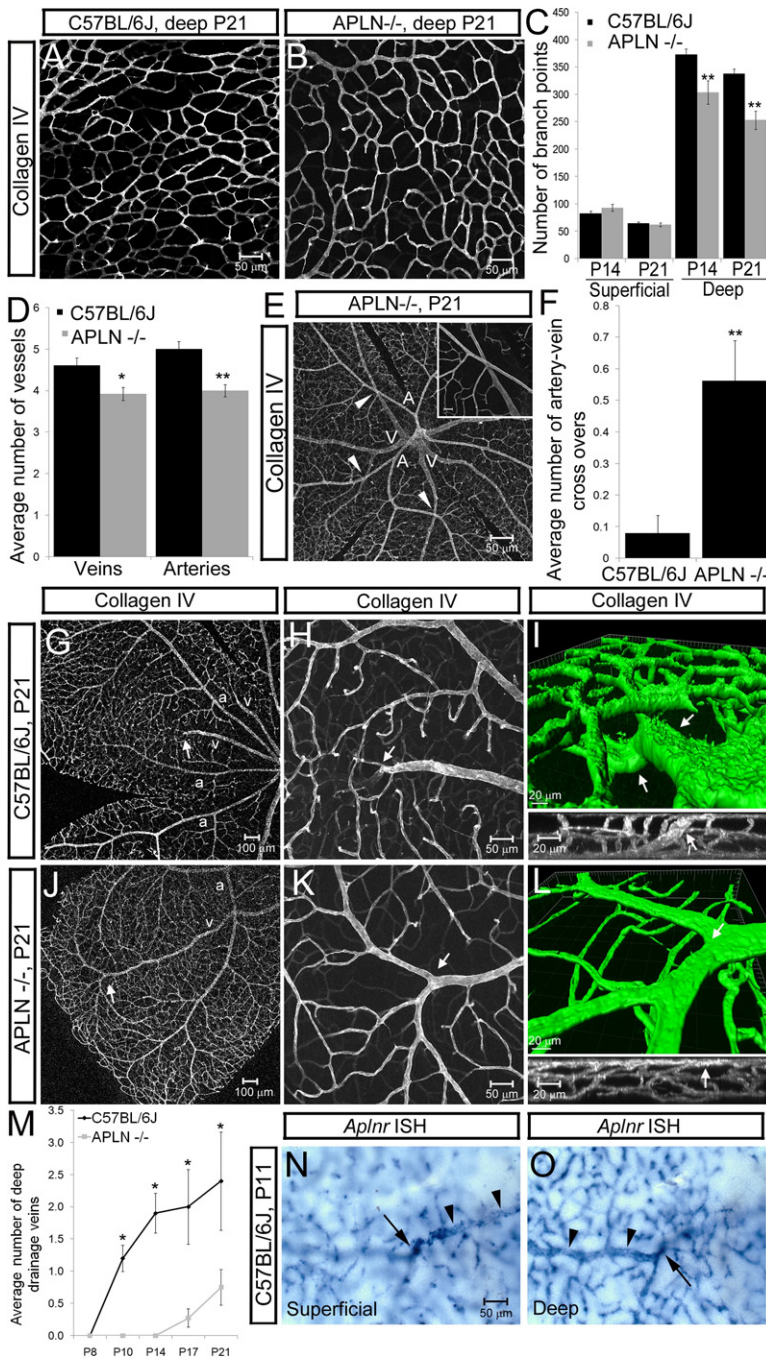


Figure 3. Developmental vascular remodeling is compromised in the *Apln*^{-/-} mouse retina. **A** and **B**: Deep vascular plexus from C57BL/6J control and *Apln*^{-/-} mice at P21. **C**: Quantification demonstrates reduced vessel branching in the deep plexus of *Apln*^{-/-} mice at P14 ($n = 5$, control; $n = 3$, *Apln*^{-/-}) and at P21 ($n = 3$). **D** and **F**: Quantification of the average number of radial veins and arteries (**D**) and arteriovenous crossings (artery over vein) (**F**) in *Apln*^{-/-} mice ($n = 32$) and C57BL/6J mice ($n = 25$) at ages P8 to P21. Data are expressed as means \pm SEM. * $P \leq 0.05$; ** $P \leq 0.01$, Student's *t*-test. **E**: Frequent arteriovenous crossings are observed in the *Apln*^{-/-} mouse. **Arrowheads** indicate arteriovenous crossings. A, arteries; V, veins. **Inset** shows a higher power magnification of a single arteriovenous crossing. **G–L**: Remodeled vein of C57BL/6J mice (**G–I**) and *Apln*^{-/-} mice (**J–L**) at P21. a, artery; v, vein. **G**: Phenotype of a radial vein (**arrow**) remodeling from the superficial to the deeper plexus, viewed from the inner retina of C57BL/6J mouse at P21. **H**: Higher power magnification of the inner retinal vascular layer showing remodeled radial vein (**arrow**). **I**: Projected serial Z-stacks (Imaris software version 7.3) of the same vessel (**arrows**), shown in the *y* axis (**top panel**) and *z* axis (**bottom panel**). **J–L**: Similar images taken from an *Apln*^{-/-} mouse, showing termination of the radial vein within the superficial plexus, where it branches, but is not remodeled into a deep drainage vein. **Arrows** indicate the bifurcation point of the radial vein. **M**: Quantification of the number of remodeled radial veins from control C57BL/6J mice and *Apln*^{-/-} mice at P8 to P21. Data are expressed as means \pm SEM ($n = 10$, control; $n = 11$, *Apln*^{-/-}). * $P \leq 0.05$, Student's *t*-test. **N** and **O**: *In situ* hybridization for *Aplnr* in C57BL/6J mice (P11). **Arrowheads** in **N** indicate the superficial radial vein and the arrow shows the point at which the radial vein remodels towards the deeper plexus to form a deep drainage venule. The **arrow** in **O** shows the same vein as in **N** emerging into the deeper plexus. **Arrowheads** in **O** indicate the deep drainage venule. Scale bars: 100 μ m (**G** and **J**); 50 μ m (**A**, **B**, **E**, **H**, **K**, **N**, and **O**); 20 μ m (**I** and **L**).

Loss of Apelin Has Little Effect on Retinal Developmental Vascular Sprouting but Does Affect Developmental Vascular Remodeling

Having established that the remodeled pathogenic vessels of the RCS rat and RD1 mouse retina express increased levels of apelin and its receptor, we next investigated whether loss of apelin affected normal retinal vascular development and remodeling. As has been previously reported,³¹ developmental retinal angiogenesis in the *Apln*^{-/-} mouse¹⁸ is largely unaffected, with only a small decrease in branching of the deeper plexus being

observed ($P < 0.01$; Figure 3, A–C). We therefore undertook a more detailed study of the vascular organization in these animals. Although whole-mounted retinas at P8 and P21 from the *Apln*^{-/-} mouse revealed no gross vascular abnormalities, in the superficial layer the total number of radial veins and arteries was decreased, relative to C57BL/6J mice ($P < 0.05$; Figure 3D). Moreover, arteriovenous crossings were observed with much greater frequency ($P < 0.01$; Figure 3, E and F). On closer examination, we also found clear evidence of abnormal remodeling of radial veins in *Apln*^{-/-} mice. In control C57BL/6J mice, veins develop in a strictly alternating

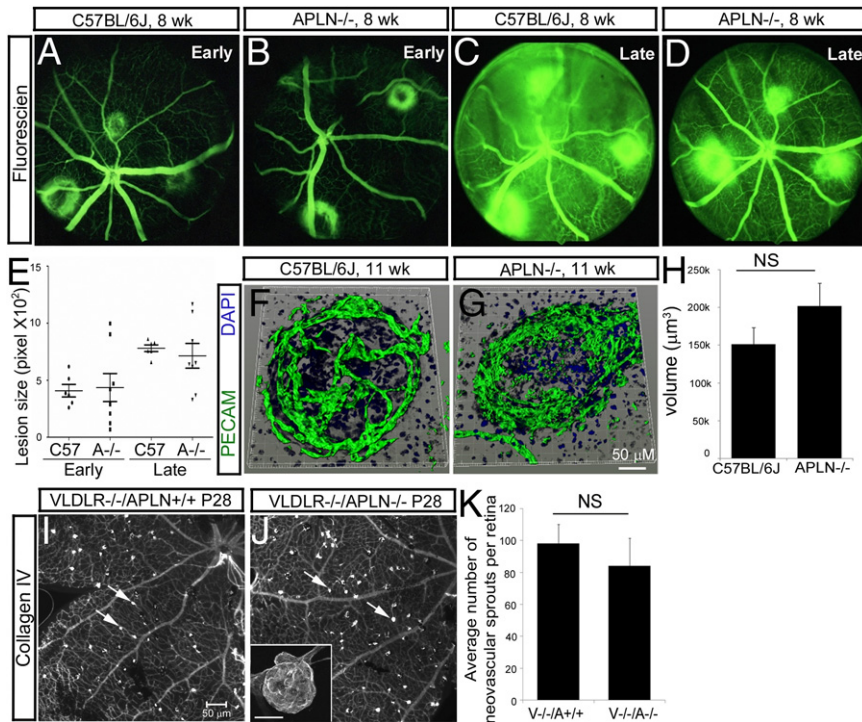


Figure 4. Apelin does not contribute to pathogenic retinal angiogenesis. **A–D:** Representative fundus fluorescein angiographs of control C57BL/6J mice and *Apln*^{−/−} mice at 2 weeks after laser-induced choroidal neovascularization. Early (90 seconds) and late (7 minutes) time points after fluorescein injection correspond to the size of the neovascular lesion and its permeability, respectively. **E:** Quantification of the area and permeability of the CNV lesion. Data are expressed as means ± SEM (*n* = 3). **F and G:** Representative three-dimensional reconstruction (Imaris software version 7.3) of CNV lesions in control C57BL/6J mice (**F**) and in *Apln*^{−/−} mice (**G**). **H:** Quantification of CNV lesion volume. Data are expressed as means ± SEM (*n* = 3). **I and J:** Representative images of retinal whole-mounts stained for vasculature in *Vldlr*^{−/−} mice (**I**) and in *Vldlr*^{−/−}/RD1 double-mutant (*R*^{−/−}) mice (**J**), showing neovascular sprouts (**arrows**); **inset** shows a single neovascular sprout. **K:** Quantification of the intraretinal neovascular sprouts in *Vldlr*^{−/−} retina (*n* = 31) and *Vldlr*^{−/−}/RD1 double-mutant (*R*^{−/−}) retina (*n* = 23). Scale bars: 50 μm (**F**, **G**, **I**, and **J**); 20 μm (**J**, **inset**).

pattern between arteries during superficial plexus development. Subsequently, as the deeper plexus develops, some (but not all) of the superficial veins are reorganized, through remodeling of existing vessels, into deeper plexus drainage veins (Figure 3, G–I; see also Supplemental Movies S1 and S2 at <http://ajp.amjpathol.org>). This leads to a relocation of veins from the superficial to the deeper plexus, although not by physical vessel translocation but rather by network remodeling. This remodeling process was disturbed in *Apln*^{−/−} mice, with most superficial veins remaining at the surface, and with dramatically reduced development of drainage veins in the deeper plexus (Figure 3, J–L). Quantification of the number of these remodeled veins per retina revealed a significant reduction in the *Apln*^{−/−} mice, relative to control animals (Figure 3M), demonstrating a prominent role for apelin in remodeling the retinal vascular plexus. To corroborate our findings we conducted *in situ* hybridization to detect *Aplnr* mRNA expression in retinal flat mounts. A positive signal was observed in the superficial radial and deep drainage retinal veins of the wild-type mouse at P11 and in the remodeled interconnecting vessels linking these two vessels (Figure 3, N and O).

Apelin Does Not Contribute to the Development of Choroidal Neovascularization or Pathogenic Intraretinal Neoangiogenesis

To ascertain whether apelin contributes to pathogenic neovascularization in the retina, we investigated whether laser-induced CNV, a feature of wet age-related macular degeneration, was attenuated in *Apln*^{−/−} mice. CNV was

induced in *Apln*^{−/−} and in control C57BL/6J mice, and fluorescein angiography was used to determine the size and permeability of the neovascular lesion. Neither at the early phase of fluorescein angiography, which reflects the size of the neovasculature, nor at the late phase, which indicates degree of fluorescein leakage, did findings differ between the *Apln*^{−/−} and control mice (Figure 4, A–E). Furthermore, analysis of lesion area (see Supplemental Figure S3 at <http://ajp.amjpathol.org>) and volume showed no difference between *Apln*^{−/−} and control mice (Figure 4, F–H). These data demonstrate that apelin does not contribute significantly to the size or permeability of the CNV lesion.

Because subretinal neovascularization in CNV is derived from the choroid, and not the retina, we next used the *Vldlr*^{−/−} mouse, which exhibits features of human retinal angiomatous proliferation, a condition found in a subset of neovascular age-related macular degeneration patients in which intraretinal neovascularization originates from the deep vascular plexus and extends toward the RPE. *Apln*^{−/−} and *Vldlr*^{−/−} mice were crossed to generate homozygous *Vldlr*/wild-type *Apln* (*V*^{−/−}/*A*^{+/+}) and homozygous knockout *Vldlr*/homozygous knockout *Apln* (*V*^{−/−}/*A*^{−/−}) littermates. These offspring were then examined for the occurrence of neovascular growths emerging from the deep vascular plexus at P28 (Figure 4, I and J). The absence of apelin had no significant effect on the number of neovascular sprouts, compared with *Vldlr*^{−/−} alone (Figure 4K). As with the CNV lesions, these observations provide strong evidence that apelin does not have any significant effect in these models of pathogenic neovascularization in the retina.

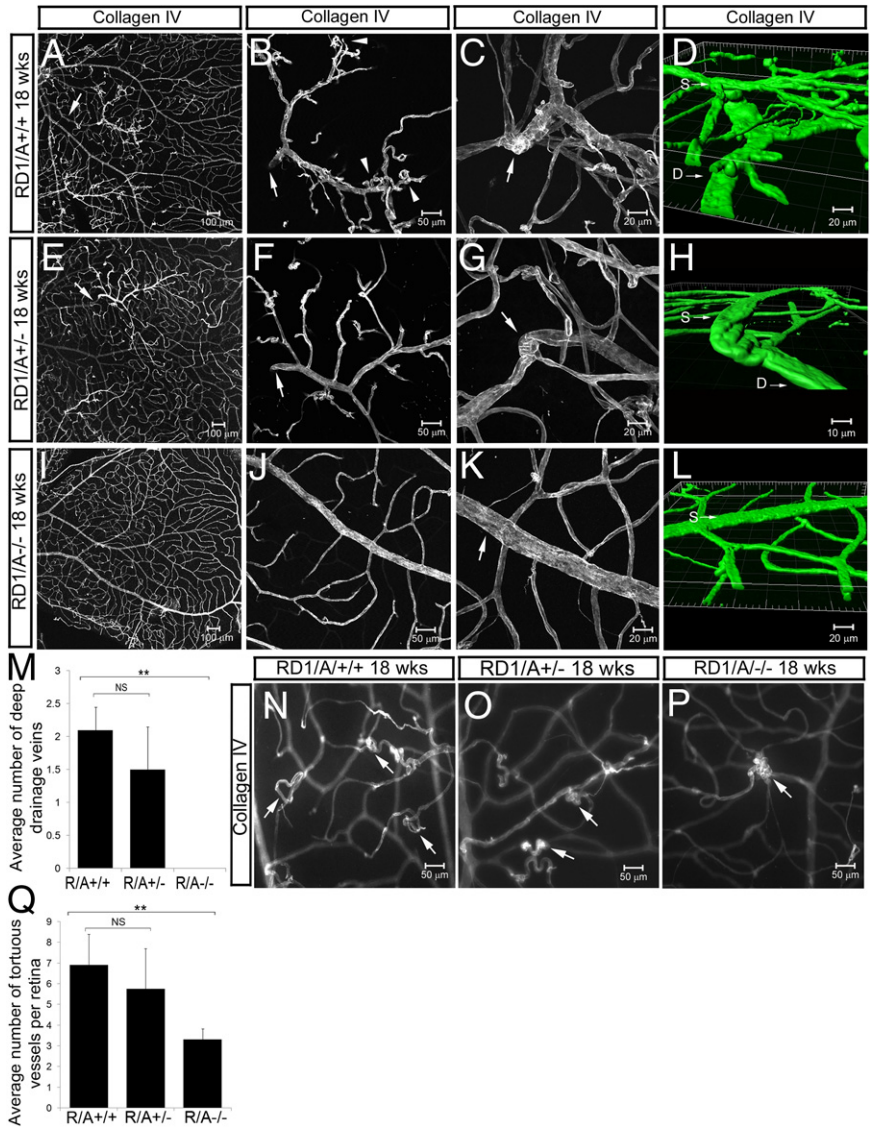


Figure 5. Loss of apelin prevents physiological radial vein remodeling in the RD1 mouse. Representative images of telangiectatic vessels associated with a deep drainage vein in an $R^{-/-}/A^{+/+}$ retina at 4.5 months of age (**A–D**) and in an $R^{-/-}/A^{+/-}$ retina from a littermate at 4.5 months of age (**E–H**). Such vascular abnormalities and drainage veins are absent in an $R^{-/-}/A^{-/-}$ retina from a littermate at 4.5 months of age (**I–L**). Retinas were visualized by epifluorescent microscopy (5 \times objective) (**A**, **E**, and **I**), by confocal microscopy showing a single section (16 \times objective) (**B**, **F**, and **J**), or by projection of a serial Z-stack (Imaris software version 7.3; 40 \times objective) (**C**, **G**, and **K**), with three-dimensional reconstructions of the Z-stack projections (**D**, **H**, and **L**). S, superficial plexus; D, deep plexus. Images are viewed from the outer retina. **A** and **E**: **Arrow** indicates the radial vein in the superficial plexus, associated with the telangiectatic vessels seen at higher magnification in **B** and **F** (**arrowheads**). **B**, **C**, **F**, and **G**: **Arrows** indicate the emergence of the drainage vein into the deeper plexus. **Arrow** in **K** shows a radial vein which has not remodelled. **M**: Quantification of remodeled radial veins with associated telangiectasis in $R^{-/-}/A^{+/+}$, $R^{-/-}/A^{+/-}$, and $R^{-/-}/A^{-/-}$ mice at 4.5 months of age ($n = 10$, $n = 4$, and $n = 11$ retinas, respectively, from five litters). Data are expressed as means \pm SEM. ****** $P \leq 0.01$, Student's *t*-test. **N–P**: Loss of apelin reduces the tortuosity of abnormal retinal vessels (**arrows**), independently of deep drainage veins. Representative images of tortuous vessels in the $R^{-/-}/A^{+/+}$ and $R^{-/-}/A^{+/-}$ retinas at 4.5 months of age (**N** and **O**), which are reduced in $R^{-/-}/A^{-/-}$ (**P**). **Q**: The average number of tortuous vessels exhibiting 360-degree turns in $R^{-/-}/A^{+/+}$, $R^{-/-}/A^{+/-}$, and $R^{-/-}/A^{-/-}$ mice ($n = 10$, $n = 4$, and $n = 11$ retinas, respectively, from five litters). Data are expressed as means \pm SEM. ****** $P \leq 0.01$, Student's *t*-test. Scale bars: 100 μ m (**A**, **E**, and **I**); 50 μ m (**B**, **F**, **J**, and **N–P**); 20 μ m (**C**, **D**, **G**, **K**, and **L**); 10 μ m (**H**).

Loss of Apelin Attenuates Pathogenic Non-Neovascular Remodeling in the Retina of the RD1 Mouse

Having established that apelin is not required for pathogenic neoangiogenesis in the CNV and *Vldlr*^{-/-} animal models, we next tested whether apelin is involved in non-neovascular remodeling induced by photoreceptor degeneration as described above. *Apln*^{-/-} and RD1 mice were crossed to generate homozygous RD1 mutant/wild-type *Apln* ($R^{-/-}/A^{+/+}$), homozygous RD1 mutant/heterozygous *Apln* ($R^{-/-}/A^{+/-}$), or homozygous RD1 mutant/homozygous knockout *Apln* ($R^{-/-}/A^{-/-}$) littermates. These progeny were examined for the occurrence of retinal vascular remodeling at 4.5 months of age. Similar to RD1 mutant animals, all crossed mice underwent thinning of the neuroretina due to photoreceptor loss (data not shown). In $R^{-/-}/A^{+/+}$ (**Figure 5, A and B**) and $R^{-/-}/A^{+/-}$ animals (**Figure 5, E and F**), tortuous telangiectatic vessels were apparent throughout the deep vascular net-

work, either as part of the capillary network or as vessels linked to the deep drainage veins, as described above for the RD1 mouse. In contrast, RD1 animals that lacked apelin ($R^{-/-}/A^{-/-}$) exhibited a marked reduction in telangiectatic vessels (**Figure 5, I and J**). Most notably, the tortuous remodeled deep drainage vessels, as described above, were completely absent (**Figure 5M**).

Examination of the spatial organization of the superficial radial veins in the $R^{-/-}/A^{+/+}$ mice revealed that they penetrated the deeper plexus in a fashion identical to that seen in the RD1 mouse (**Figure 5, C and D**). $R^{-/-}/A^{+/-}$ mice also had remodeled drainage veins (**Figure 5, G and H**). Similar to the *Apln*^{-/-} mouse, the $R^{-/-}/A^{-/-}$ also exhibited a dramatic reduction in remodeled drainage veins (**Figure 5, K and L**). Loss of these large remodeled drainage veins may therefore explain the absence of telangiectatic deep drainage vessels observed in the $R^{-/-}/A^{-/-}$ mice. However, in the $R^{-/-}/A^{+/+}$ mouse a significant number of telangiectatic vessels was observed in the surviving intermediate/deep capillary

plexus, which was not affected. We therefore investigated whether depleting apelin reduced the number of telangiectatic capillaries in this cohort of vessels, because these telangiectatic capillaries would be independent of the loss of deep draining veins. In the $R^{-/-}/A^{+/+}$ and $R^{-/-}/A^{+/-}$ mice, numerous telangiectatic capillaries were observed (Figure 5, N and O). In the $R^{-/-}/A^{-/-}$ mice, abnormal capillaries were also observed, but these exhibited reduced and negligible tortuosity, compared with those seen in the $R^{-/-}/A^{+/+}$ mice, respectively (Figure 5, O and P). When the level of tortuosity was quantified by enumerating the number of vessels with 360-degree turns per retina, the degree of telangiectasia in the $R^{-/-}/A^{-/-}$ mice was substantially reduced (Figure 5Q). These data provide strong evidence that apelin regulates the pathogenic non-neovascular remodeling of microvessels, particularly with respect to telangiectasia.

Discussion

Gene expression analysis of the vasculature of two animal models of retinal degeneration with associated vascular remodeling revealed a number of differentially expressed genes common to both pathologies. Two of these genes, encoding the small secreted peptide ApIn and its cognate receptor ApInr, were significantly up-regulated, relative to control vessels, and were selected for further investigation. Apelin exists as an inactive 77-amino-acid preproprotein and as various active cleavage products, of which apelin-13 is the most biologically active. The apelin receptor, for which apelin is the only known ligand, is a G protein-coupled receptor (GPCR) that associates with both $G_{\alpha i}$ and G_q heterotrimeric G proteins to induce activation of Akt/ERK and PLC, respectively.^{32,33} Current data suggest that the vascular endothelium is a major target of apelin signaling, with various downstream effects such as increased cell division and migration^{27,34} and eNOS activation and NO production.^{35,36} In addition, apelin has been reported to modulate developmental angiogenesis,^{25,26,28,31,34,37} pathogenic angiogenesis,^{26,29,37,38,39,40,41} and angiogenesis in *in vitro* assays.^{27,34} Although the overall interpretation of many of these studies is that apelin is involved in angiogenesis, close inspection reveals that the evidence is far from conclusive. For example, many studies do not distinguish between sprouting angiogenesis and vascular remodeling. Thus, the common readouts used to assess angiogenesis, such as vessel density, branch points and vascular structural abnormalities, may be altered as result of vascular remodeling alone (eg, increased or decreased vessel pruning). Moreover, many studies simply demonstrate a correlation between ApIn/ApInr expression and angiogenesis but do not demonstrate a causal link and others are based on imperfect *in vitro* cell culture models. Similarly, in the clinical setting, apelin expression is significantly increased in the vitreous of patients with proliferative diabetic retinopathy,^{42,43} but again both neovascularization and vascular remodeling occur. More consistent with our findings is the observation that apelin is necessary for normal vessel caliber

development in various tissues.^{44,45} Nevertheless, as discussed below, the apelinergic pathway may contribute to angiogenesis, especially in the context of modifying the VEGF response.

We observed that ApIn and ApInr are coexpressed in the retinal microvasculature, implying the presence of autocrine signaling. Although ApInr expression in the retina is restricted to the retinal vessels, demonstrating the vasculature as the primary target of apelin activity, some apelin expression was also observed in the nonvascular compartment. This latter finding may be due to expression in Müller cells,⁴⁶ which is pertinent, given that Müller cell end-feet associate closely with the inner retinal vasculature and are likely to play an important part in determining vascular function. In the vasculature of the RCS and RD1 rodent models of retinal degeneration, the levels of apelin and its receptor were significantly up-regulated, which is consistent with them being under similar regulatory control. In many tissues, the expression patterns of ApIn and ApInr have been shown to be closely aligned, with *ApIn* and *ApInr* gene expression coordinated through SP1-mediated transcriptional regulation.^{47,48} Of note, it has been reported that a single-nucleotide polymorphism at an SP1 binding site in the 5' flanking region of the *ApInr* gene induces ApInr activity and confers an increased risk of cerebral infarct.⁴⁷ Although the mechanism is currently unknown, we might speculate that increased microvascular tortuosity due to ApIn/ApInr-mediated remodeling may predispose to increased infarct susceptibility and hemorrhage in the brain.

Earlier reports have implicated ApIn and ApInr in retinal blood vessel development³¹ with enhanced mRNA expression at the leading edge of the superficial plexus as it develops toward the periphery.^{25,28,49} In the *ApIn*^{-/-} mouse, however, only minor transient delays in retinal vascular development have been reported.³¹ We observed reduced branching of the deeper plexus at P14 and P21 in *ApIn*^{-/-} mice, as well as a significant decrease in the number of radial arteries and veins and an increase in the frequency of arteriovenous crossings, relative to C57BL/6J controls. Most notable, however, was the novel observation that *ApIn*^{-/-} mice have reduced remodeled radial veins. In control animals, an average of 2.1 radial veins in the superficial plexus remodel and become integrated into the deeper vascular plexus as it develops, becoming deep drainage venules.¹⁵ The mechanism through which this occurs is currently unclear, but given that the deeper plexus arises from all radial veins, and not just the subset that remodels downward, it seems likely that this is a regulated process. Our data, therefore, support our hypothesis that apelin is an important regulator of this aspect of developmental vascular remodeling. Notably, other deep venules that result from branching from the radial veins were unaffected by loss of apelin, because they were present in both C57BL/6J and *ApIn*^{-/-} mice.

Having established that apelin is required for some elements of developmental vascular remodeling in the retina, the question arose of whether, as suggested by the gene expression data, apelin is also required for pathogenic non-neovascular remodeling. The RD1 mouse is an ani-

mal model of retinal degeneration that exhibits retinal vascular telangiectasia in the absence of any significant neoangiogenesis. We therefore generated *Apln*-knockout mice on the RD1 background to test whether the apelinergic pathway contributes to telangiectatic vascular remodeling. These mice exhibited a striking loss of telangiectatic vessels. Although the loss of some telangiectatic deep venules may result from the failure to develop remodeled veins, the number of telangiectatic capillaries not associated with these vessels was also reduced substantially. This provides compelling evidence that apelin is essential for pathogenic non-neovascular remodeling in the retina.

Apelin has been implicated in pathogenic neoangiogenesis.^{26,27,29,37-41} To gain further insight into the role of apelin in retinal vascular pathology, we investigated the role of apelin in the CNV and *Vldlr*^{-/-} models of retinal neovascularization. Surprisingly, we observed no difference in the extent of CNV in *Apln*^{-/-} mice, relative to wild-type controls; similarly, in the *Apln/Vldlr* double-knockout mice the number of intraretinal neovascular growths was not significantly different from that observed in the *Vldlr*^{-/-} mice. These data appear to be at odds with the recently reported effects of apelin in the mouse model of oxygen-induced ischemic retinopathy. The hypoxia-induced increase in retinal capillary density is attenuated at P15 and P17 in *Apln*-knockout mice.³⁹ However, retinal capillary density is already reduced in these mice at the age at which oxygen-induced ischemic retinopathy is induced³¹ (our data not shown), making it unclear whether the effects are due primarily to loss of apelin or to the underlying delay in retinal vascular development in these animals. Furthermore, it is important to note that the effects are not permanent, because vessel density reaches parity between the wild type and *Apln*^{-/-} by P84.³¹ Alternatively, this discrepancy may reveal that, as is the case with *TGFβ*, the outcome of apelin signaling is extremely dependent on context. It may therefore be proposed that, in the presence of low VEGF expression (as in the RD1 mouse retina), the apelinergic pathway cannot independently promote sprouting angiogenesis and that its primary role is to drive non-neovascular modifications. In the presence of significantly elevated VEGF, however, apelin can either contribute to pathogenic vascular sprouting or have no effect, depending on the relative contribution of other differentially activated costimulatory pathways. This is supported by the finding that apelin exerts its effect on a corneal angiogenesis assay primarily through a cooperative process involving VEGF or FGF2.³¹ It is entirely feasible, therefore, that in retinal pathological angiogenesis, in which hypoxia is the predominant driving factor, both apelin and VEGF combine to determine the extent of new blood vessel growth,^{31,45} whereas when additional contributing factors are involved, such as in CNV and in the *Vldlr*^{-/-} mouse, the role of apelin in neovascularization is diminished. Our data, however, suggest that in the retina apelin is involved predominantly in developmental and pathogenic non-neovascular remodeling, because it has a marginal effect in physiological angiogenesis and no effect on patholog-

ical neovascularization observed in laser-induced CNV or *Vldlr*^{-/-} mice.

Over several decades, a great deal of information has been gathered describing the factors that regulate developmental, physiological, and pathological sprouting angiogenesis. Much less, however, is understood of the factors that control non-neovascular remodeling, despite its clear pathogenic importance. With the present study, we have demonstrated that apelin and its cognate receptor *Aplnr* are involved in remodeling of the vasculature in retinal development and disease and in the latter case may represent a novel target for therapeutic intervention.

References

1. Fruttiger M: Development of the mouse retinal vasculature: angiogenesis versus vasculogenesis. *Invest Ophthalmol Vis Sci* 2002, 43:522-527
2. Qazi Y, Maddala S, Ambati BK: Mediators of ocular angiogenesis. *J Genet* 2009, 88:495-515
3. Yannuzzi LA, Bardal AM, Freund KB, Chen KJ, Eandi CM, Blodi B: Idiopathic macular telangiectasia. *Arch Ophthalmol* 2006, 124:450-460
4. Chew EY, Murphy RP, Newsome DA, Fine SL: Parafoveal telangiectasis and diabetic retinopathy. *Arch Ophthalmol* 1986, 104:71-75
5. Black GC, Perveen R, Bonshek R, Cahill M, Clayton-Smith J, Lloyd IC, McLeod D: Coats' disease of the retina (unilateral retinal telangiectasis) caused by somatic mutation in the NDP gene: a role for norrin in retinal angiogenesis. *Hum Mol Genet* 1999, 8:2031-2035
6. Maugé-Fayssé M, Vuillaume M, Quaranta M, Moullan N, Angèle S, Friesen MD, Hall J: Idiopathic and radiation-induced ocular telangiectasia: the involvement of the ATM gene. *Invest Ophthalmol Vis Sci* 2003, 44:3257-3262
7. Lavin MF: Ataxia-telangiectasia: from a rare disorder to a paradigm for cell signalling and cancer [Erratum in *Nat Rev Mol Cell Biol* 2008;9(12). doi: 10.1038/nrm2514]. *Nat Rev Mol Cell Biol* 2008, 9:759-769
8. Marc RE, Jones BW, Watt CB, Strettoi E: Neural remodeling in retinal degeneration. *Prog Retin Eye Res* 2003, 22:607-655
9. Bourne MC, Campbell DA, Tansley K: Hereditary degeneration of the rat retina. *Br J Ophthalmol* 1938, 22:613-623
10. D'Cruz PM, Yasumura D, Weir J, Matthes MT, Abderrahim H, LaVail MM, Vollrath D: Mutation of the receptor tyrosine kinase gene *Mertk* in the retinal dystrophic RCS rat. *Hum Mol Genet* 2000, 9:645-651
11. Wang S, Villegas-Pérez MP, Holmes T, Lawrence JM, Vidal-Sanz M, Hurtado-Montalban N, Lund RD: Evolving neurovascular relationships in the RCS rat with age. *Curr Eye Res* 2003, 27:183-196
12. Blanks JC, Johnson LV: Vascular atrophy in the retinal degenerative rd mouse. *J Comp Neurol* 1986, 254:543-553
13. Bowes C, Li T, Danciger M, Baxter LC, Applebury ML, Farber DB: Retinal degeneration in the rd mouse is caused by a defect in the beta subunit of rod cGMP-phosphodiesterase. *Nature* 1990, 347: 677-680
14. Otani A, Dorrell MI, Kinder K, Moreno SK, Nusinowitz S, Banin E, Heckenlively J, Friedlander M: Rescue of retinal degeneration by intravitreally injected adult bone marrow-derived lineage-negative hematopoietic stem cells. *J Clin Invest* 2004, 114:765-774
15. Wang S, Villegas-Pérez MP, Vidal-Sanz M, Lund RD: Progressive optic axon dystrophy and vascular changes in rd mice. *Invest Ophthalmol Vis Sci* 2000, 41:537-545
16. Dorrell MI, Friedlander M: Mechanisms of endothelial cell guidance and vascular patterning in the developing mouse retina. *Prog Retin Eye Res* 2006, 25:277-295
17. Heckenlively JR, Hawes NL, Friedlander M, Nusinowitz S, Hurd R, Davisson M, Chang B: Mouse model of subretinal neovascularization with choroidal anastomosis. *Retina* 2003, 23:518-522
18. Kuba K, Zhang L, Imai Y, Arab S, Chen M, Maekawa Y, Leschnik M, Leibbrandt A, Markovic M, Schwaighofer J, Beetz N, Musialek R, Neely GG, Komnenovic V, Kolm U, Metzler B, Ricci R, Hara H, Meixner A, Nghiem M, Chen X, Dawood F, Wong KM, Sarao R,

- Cukerman E, Kimura A, Hein L, Thalhammer J, Liu PP, Penninger JM: Impaired heart contractility in Apelin gene-deficient mice associated with aging and pressure overload. *Circ Res* 2007, 101:e32–e42
19. Balaggan KS, Binley K, Esapa M, MacLaren RE, Iqbal S, Duran Y, Pearson RA, Kan O, Barker SE, Smith AJ, Bainbridge JW, Naylor S, Ali RR: EIAV vector-mediated delivery of endostatin or angiostatin inhibits angiogenesis and vascular hyperpermeability in experimental CNV. *Gene Ther* 2006, 13:1153–1165
 20. Gimenez E, Montoliu L: A simple polymerase chain reaction assay for genotyping the retinal degeneration mutation (Pdeb(rd1)) in FVB/N-derived transgenic mice. *Lab Anim* 2001, 35:153–156
 21. Offman J, Jina N, Theron T, Pallas J, Hubank M, Lehmann A: Transcriptional changes in trichothiodystrophy cells. *DNA Repair (Amst)* 2008, 7:1364–1371
 22. Zambarakji HJ, Keegan DJ, Holmes TM, Halfyard AS, Villegas-Perez MP, Charteris DG, Fitzke FW, Greenwood J, Lund RD: High resolution imaging of fluorescein patterns in RCS rat retinæ and their direct correlation with histology. *Exp Eye Res* 2006, 82:164–171
 23. Li C, Huang Z, Kingsley R, Zhou X, Li F, Parke DW 2nd, Cao W: Biochemical alterations in the retinas of very low-density lipoprotein receptor knockout mice: an animal model of retinal angiomatous proliferation. *Arch Ophthalmol* 2007, 125:795–803
 24. Hu W, Jiang A, Liang J, Meng H, Chang B, Gao H, Qiao X: Expression of VLDLR in the retina and evolution of subretinal neovascularization in the knockout mouse model's retinal angiomatous proliferation. *Invest Ophthalmol Vis Sci* 2008, 49:407–415
 25. del Toro R, Prahst C, Mathivet T, Siegfried G, Kaminker JS, Larrivee B, Breant C, Duarte A, Takakura N, Fukamizu A, Penninger J, Eichmann A: Identification and functional analysis of endothelial tip cell-enriched genes. *Blood* 2010, 116:4025–4033
 26. Kälin RE, Kretz MP, Meyer AM, Kispert A, Heppner FL, Brändli AW: Paracrine and autocrine mechanisms of apelin signaling govern embryonic and tumor angiogenesis. *Dev Biol* 2007, 305:599–614
 27. Kasai A, Shintani N, Oda M, Kakuda M, Hashimoto H, Matsuda T, Hinuma S, Baba A: Apelin is a novel angiogenic factor in retinal endothelial cells. *Biochem Biophys Res Commun* 2004, 325:395–400
 28. Saint-Geniez M, Masri B, Malecaze F, Knibiehler B, Audigier Y: Expression of the murine msr/apj receptor and its ligand apelin is upregulated during formation of the retinal vessels. *Mech Dev* 2002, 110:183–186
 29. Sorli SC, Le GS, Knibiehler B, Audigier Y: Apelin is a potent activator of tumour neoangiogenesis. *Oncogene* 2007, 26:7692–7699
 30. Kumar M, Tyagi N, Moshal KS, Sen U, Pushpakumar SB, Vacek T, Lominadze D, Tyagi SC: GABAA receptor agonist mitigates homocysteine-induced cerebrovascular remodeling in knockout mice. *Brain Res* 2008, 1221:147–153
 31. Kasai A, Shintani N, Kato H, Matsuda S, Gomi F, Haba R, Hashimoto H, Kakuda M, Tano Y, Baba A: Retardation of retinal vascular development in apelin-deficient mice. *Arterioscler Thromb Vasc Biol* 2008, 28:1717–1722
 32. Bai B, Tang J, Liu H, Chen J, Li Y, Song W: Apelin-13 induces ERK1/2 but not p38 MAPK activation through coupling of the human apelin receptor to the Gi2 pathway. *Acta Biochim Biophys Sin (Shanghai)* 2008, 40:311–318
 33. Masri B, Morin N, Pedebnarde L, Knibiehler B, Audigier Y: The apelin receptor is coupled to Gi1 or Gi2 protein and is differentially desensitized by apelin fragments. *J Biol Chem* 2006, 281:18317–18326
 34. Cox CM, D'Agostino SL, Miller MK, Heimark RL, Krieg PA: Apelin, the ligand for the endothelial G-protein-coupled receptor, APJ, is a potent angiogenic factor required for normal vascular development of the frog embryo. *Dev Biol* 2006, 296:177–189
 35. Ishida J, Hashimoto T, Hashimoto Y, Nishiwaki S, Iguchi T, Harada S, Sugaya T, Matsuzaki H, Yamamoto R, Shiota N, Okunishi H, Kihara M, Umemura S, Sugiyama F, Yagami K, Kasuya Y, Mochizuki N, Fukamizu A: Regulatory roles for APJ, a seven-transmembrane receptor related to angiotensin-type 1 receptor in blood pressure in vivo. *J Biol Chem* 2004, 279:26274–26279
 36. Zhong JC, Yu XY, Huang Y, Yung LM, Lau CW, Lin SG: Apelin modulates aortic vascular tone via endothelial nitric oxide synthase phosphorylation pathway in diabetic mice. *Cardiovasc Res* 2007, 74:388–395
 37. Sorli SC, van den Berghe L, Masri B, Knibiehler B, Audigier Y: Therapeutic potential of interfering with apelin signalling. *Drug Discov Today* 2006, 11:1100–1106
 38. Berta J, Kenessey I, Dobos J, Tovari J, Klepetko W, Jan AH, Hegedus B, Renyi-Vamos F, Varga J, Lorincz Z, Paku S, Ostoros G, Rozsas A, Timar J, Dome B: Apelin expression in human non-small cell lung cancer: role in angiogenesis and prognosis. *J Thorac Oncol* 2010, 5:1120–1129
 39. Kasai A, Ishimaru Y, Kinjo T, Satooka T, Matsumoto N, Yoshioka Y, Yamamuro A, Gomi F, Shintani N, Baba A, Maeda S: Apelin is a crucial factor for hypoxia-induced retinal angiogenesis. *Arterioscler Thromb Vasc Biol* 2010, 30:2182–2187
 40. Kunduzova O, Alet N, Delesque-Touchard N, Millet L, Castan-Laurell I, Muller C, Dray C, Schaeffer P, Herault JP, Savi P, Bono F, Valet P: Apelin/APJ signaling system: a potential link between adipose tissue and endothelial angiogenic processes. *FASEB J* 2008, 22:4146–4153
 41. Tiani C, Garcia-Pras E, Mejias M, de GA, Berzigotti A, Bosch J, Fernandez M: Apelin signaling modulates splanchnic angiogenesis and portosystemic collateral vessel formation in rats with portal hypertension. *J Hepatol* 2009, 50:296–305
 42. Qian J, Lu Q, Tao Y, Jiang YR: Vitreous and plasma concentrations of apelin and vascular endothelial growth factor after intravitreal bevacizumab in eyes with proliferative diabetic retinopathy. *Retina* 2011, 31:161–168
 43. Tao Y, Lu Q, Jiang YR, Qian J, Wang JY, Gao L, Jonas JB: Apelin in plasma and vitreous and in fibrovascular retinal membranes of patients with proliferative diabetic retinopathy. *Invest Ophthalmol Vis Sci* 2010, 51:4237–4242
 44. Kidoya H, Naito H, Takakura N: Apelin induces enlarged and non-leaky blood vessels for functional recovery from ischemia. *Blood* 2010, 115:3166–3174
 45. Kidoya H, Ueno M, Yamada Y, Mochizuki N, Nakata M, Yano T, Fujii R, Takakura N: Spatial and temporal role of the apelin/APJ system in the caliber size regulation of blood vessels during angiogenesis. *EMBO J* 2008, 27:522–534
 46. Loewen N, Chen J, Dudley VJ, Sarthy VP, Mathura Jr Jr: Genomic response of hypoxic Müller cells involves the very low density lipoprotein receptor as part of an angiogenic network. *Exp Eye Res* 2009, 88:928–937
 47. Hata J, Matsuda K, Ninomiya T, Yonemoto K, Matsushita T, Ohnishi Y, Saito S, Kitazono T, Ibayashi S, Iida M, Kiyohara Y, Nakamura Y, Kubo M: Functional SNP in an Sp1-binding site of AGTRL1 gene is associated with susceptibility to brain infarction. *Hum Mol Genet* 2007, 16:630–639
 48. O'Carroll AM, Lolait SJ, Howell GM: Transcriptional regulation of the rat apelin receptor gene: promoter cloning and identification of an Sp1 site necessary for promoter activity. *J Mol Endocrinol* 2006, 36:221–235
 49. Saint-Geniez M, Argence CB, Knibiehler B, Audigier Y: The msr/apj gene encoding the apelin receptor is an early and specific marker of the venous phenotype in the retinal vasculature. *Gene Expr Patterns* 2003, 3:467–472